https://doi.org/10.5194/egusphere-2024-4165
Preprint. Discussion started: 16 January 2025

On the presence of high nitrite (NO_2^-) in coarse particles at Mt. Qomolangma

Zhongyi Zhang[1, 2], Chunxiang Ye[3], Yichao Wu[1], Tao Zhou[4], Pengfei Chen[5,6], Shichang Kang[5,6], Chong Zhang[3], Zhuang Jiang[1], Lei Geng[1, 2, 4*]

[1]Deep Space Exploration Laboratory/School of Earth and Space Sciences, University of Science and Technology of China, Hefei 230026, Anhui, China

[2]CAS Center for Excellence in Comparative Planetology, University of Science and Technology of China, Hefei 230026, Anhui, China

[3]SKL-ESPC & SEPKL-AERM, College of Environmental Sciences and Engineering, and Center for Environment and Science, Peking University, Beijing 100871, China

[4]National Key Laboratory of Deep Space Exploration, Hefei, 230088, Anhui, China.

[5]Key Laboratory of Cryospheric Science and Frozen Soil Engineering, Northwest Institute of Eco-Environment and Resources, Chinese Academy of Sciences; Lanzhou, 730000, Gansu, China

[6]University of Chinese Academy of Sciences; Beijing, 100049, China

* *Correspondence to*: Lei Geng (Email: genglei@ustc.edu.cn; Tel: +86-0551-63600015)

https://doi.org/10.5194/egusphere-2024-4165
Preprint. Discussion started: 16 January 2025

Abstract

Atmospheric reactive nitrogen cycling is crucial for maintaining the atmospheric oxidation capacity of background atmosphere on the Tibetan Plateau, with nitrous acid (HONO) and particulate nitrite (NO_2^-) as important intermediates. During an eleven-day field campaign at the Base Camp of Mt. Qomolangma in spring of 2022, we observed significant enrichment of NO_2^- in total suspended particulate (TSP) with a mean concentration of 375 ± 386 ng m^{-3}, while NO_2^- was absent in fine particles ($PM_{2.5}$). The comparison revealed that NO_2^- predominately exists in coarse particles. Local surface soil at the sampling site also exhibited high levels of NO_2^-, with $\delta^{15}N$ value similar to NO_2^- in TSP. This similarity suggests that wind-blown soil is probably the primary source of NO_2^- in TSP, accounting for the background levels. While concentration changes of water-soluble inorganic ions in TSP and $PM_{2.5}$ in response to shifts in air mass back-trajectories imply that atmospheric pollutants transported from South Asia may further elevate the NO_2^-, the specific mechanisms of long-range transport resulting in NO_2^- accumulation in TSP rather than $PM_{2.5}$ remain unknown and need to be investigated. Our results reveal an overlooked source of atmospheric NO_2^-, i.e., soil NO_2^-, and highlight in remote regions such as Tibet where other sources are limited, wind-blown soil may serve as an important source of atmospheric NO_2^-. Once lofted into the atmosphere, NO_2^- may readily participate in atmospheric reactive nitrogen cycling through gas-particle partitioning or photolysis, leading to the production of HONO, OH and NO and thereby influencing oxidation chemistry.

https://doi.org/10.5194/egusphere-2024-4165
Preprint. Discussion started: 16 January 2025

1 Introduction

The Himalayas-Tibetan Plateau (HTP) represents one of the most important geomorphologically cryospheric regions, boasting high abundance of alpine glaciers and extensive areas of high-altitude snow cover (Kehrwald et al., 2008; Yao et al., 2012; Kang et al., 2019). The melting of snow cover and glacier ice holds immense importance as crucial freshwater resources for over 1.4 billion people in Asia, earning HTP the title as the "Water Tower of Asia" (Immerzeel et al., 2010). However, the enhanced warming rate in the Tibetan Plateau (TP, ~ 0.30℃ per decade) has resulted in a rapid and alarming increase in glacier melting over the past decade, significantly affecting the climate, hydrological cycles, and ecosystems at local and global scales (Immerzeel et al., 2010; Xu et al., 2009; Lau et al., 2010). Persistently increased aerosol loadings and greenhouse gas in TP region account for the increased warming rate (Kang et al., 2019; Lau et al., 2010; Lüthi et al., 2015). More importantly, once deposited on the surface of snow cover and glacier ice, the aerosol, especially these light-absorbing components (i.e., black carbon, dust) contribute significantly to the rapid glacial retreat (Xu et al., 2009; Zhao et al., 2020).

Atmospheric oxidation capacity (AOC) regulates the formation of secondary aerosol and the removal of trace gases including CH_4 (Wang et al., 2023; Ye et al., 2023; Ye et al., 2016; Andersen et al., 2023), therefore acting as a critical link between atmospheric pollution and cryospheric changes. Previous study have suggested strong solar radiation, high O_3 and relatively high water vapor dominate the relatively strong AOC over the TP (Lin et al., 2008). Recent field campaign further highlighted the rapid reactive nitrogen cycling, with N(III) species (i.e., HONO) as the intermediate, also plays an important role in maintaining the strong AOC in TP (Wang et al., 2023). For example, *Wang et al.* reported high-than-expected HONO (~30 ± 13 pptv) in the Namco station, a typical background site in the middle of TP, with soil emission and particulate nitrate photolysis as the dominant sources (Wang et al., 2023). Interestingly, relatively high levels of nitrite (NO_2^-) in total suspended particulate (TSP) have also been reported from remote sites of TP, i.e., in a forest site in the Southeast Tibet (~ 140 ng m^{-3}) and at the Qomolangma monitoring station (QOMS, ~ 60 ng m^{-3}) (Bhattarai et al., 2019; Bhattarai et al., 2023). Such high levels of particulate NO_2^- may also contribute to the strong AOC in TP, either via directly photolysis to produce NO_x (Jacobi et al., 2014)

https://doi.org/10.5194/egusphere-2024-4165
Preprint. Discussion started: 16 January 2025

or indirectly serve as an important source of HONO through gas-particle partitioning (R1). However, the sources and formation mechanisms for the relatively high level of atmospheric NO_2^- observed in the TP remain unclear.

$$HONO_{(g)} \leftrightarrow HONO_{(aq)} \leftrightarrow NO_2^-{}_{(aq)} + H^+_{(aq)} \quad (R1)$$

$$HONO_{(aq)} + H^+_{(aq)} \leftrightarrow H_2ONO^+_{(aq)} \quad (R2)$$

$$HONO + h\upsilon\ (300\ nm < \lambda < 405\ nm) \rightarrow NO + OH \quad (R3)$$

The stable nitrogen and oxygen isotopic compositions ($\delta^{15}N$, $\delta^{18}O$, and $\Delta^{17}O$; where $\delta = (R_{sample}/R_{reference} - 1) \times 1000‰$ and with R denoting the $^{15}N/^{14}N$, $^{18}O/^{16}O$, and $^{17}O/^{16}O$ ratios; $\Delta^{17}O = \delta^{17}O - 0.52 \times \delta^{18}O$) may provide diagnostic information regarding the sources and formation pathways of atmospheric nitrite. Similar isotopic approaches have been widely used to explore the nitrate (NO_3^-) sources (Morin et al., 2008; Zong et al., 2020; Geng et al., 2014; Fang et al., 2011; Hastings et al., 2003; Zhang et al., 2022; Zhang et al., 2021b; Liu et al., 2018; Felix and Elliott, 2014; Miller et al., 2018). Considering that atmospheric NO_2^- may share similar sources and formation pathways with NO_3^-, the specific NO_2^- formation pathways are expected to be characterized by distinct oxygen or nitrogen isotopic endmembers, despite reports on the atmospheric NO_2^- isotopic compositions are rare. For instance, NO_2^- produced from the photolysis of particulate NO_3^- may possess very negative $\delta^{15}N$ values compared to NO_3^-, analogous to the pronounced nitrogen isotope fractionation effects associated with snow nitrate photolysis (Erbland et al., 2013), while the $\Delta^{17}O$ of NO_2^- is expected to closely resemble that of NO_3^- as the oxygen atom in NO_2^- is imparted from NO_3^-, unless significant oxygen atom exchange between NO_2^- and aerosol water occurs. The $\Delta^{17}O$ of NO_2^- (and HONO) from primary emission sources is expected to be negligible, while that generated from heterogeneous reactions of NO_2 on the aerosol surface would be characterized by positive $\Delta^{17}O$ values depending on the degree of NO_2^- and aerosol water oxygen isotope exchange. These unique isotopic fingerprints may be utilized in distinguishing the sources and formation pathways of atmospheric NO_2^-.

To gain insight into the sources and/or formation mechanisms of atmospheric NO_2^- in the pristine environment of TP, we collected the TSP and fine particulate matter ($PM_{2.5}$) synchronously at the Base Camp, the north slope of the Mt. Qomolangma during the campaign of "Earth Summit

https://doi.org/10.5194/egusphere-2024-4165
Preprint. Discussion started: 16 January 2025

Mission-2022" scientific expedition from April 24th to May 6th, 2022, with additional surface soil samples collected in May, 2023. The NO_2^- concentration and multi-isotopic signatures ($\delta^{15}N$, $\delta^{18}O$, and $\Delta^{17}O$) in aerosol and surface soil were then determined in order to evaluate the potential sources of atmospheric NO_2^-. Additionally, the potential environmental implication of atmospheric nitrite was explored in the term of atmospheric oxidation capacity at this pristine environment.

2 Material and Method

2.1 Site description

The Base Camp is located in the middle of the Rongbuk valley (86.85 °E, 28.14 °N), situated ~5200 m above sea level (m a.s.l) on the north slope of the Mt. Qomolangma (Zou et al., 2008; Zhu et al., 2006). The surrounding surface consists of loosed soil, gravel, broken rocks of various sizes, with sparse vegetation due to the semi-arid status (Ming et al., 2007; Zou et al., 2008). Rongbuk valley is characterized by a depth of ~1000 m and a floor width of ~1000 m, with elevations of the surrounding mountains exceeding 6000 m on both sides (Zou et al., 2008). Attributed to the unique topography, the local air circulation is dominated by mountain and valley breezes. The predominant wind regime is the katabatic flow of southerly and southeasterly, which is typically persists from noon to midnight (Zhu et al., 2006; Zou et al., 2008; Zhou et al., 2011). The nearest accessible area for residents and visitors is at least 2 km north of the Base Camp. During the campaign, electricity and natural gases were routinely used for cooking and hot water production. There were intermittent vehicle exhaust emissions around the station during daytime for the daily necessaries supporting, i.e., water and food. To minimize the influence of local anthropogenic activities on sampling, the instruments were set in the southwest (upwind direction) and approximately 100 m away from the living space of the Base Camp. The anthropogenic influence on the sampling is expected to be minimal.

2.2 Field campaign and sample collection

From April 26th to May 6th, 2022, TSP samples were collected simultaneously with NO_2 using a homemade denuder-filter system (Zhou et al., 2022). A polytetrafluoroethylene (PTFE) sleeve is used to assemble the homemade denuder with the filter pack, flowmeter, and pump. The filter pack was placed in the front of the denuder. All connections between the various parts of the sampling

https://doi.org/10.5194/egusphere-2024-4165
Preprint. Discussion started: 16 January 2025

apparatus are made using 3/8″ Teflon tubing. A detailed description of the sampling apparatus can be found in our previous report (Zhou et al., 2022). Whatman quartz filter (circles, diam. 47mm, pre-heated at 400 ℃ for 3 h before use) was placed into the filter pack to collect TSP sample. In the present study, the collected bulk aerosol can be regarded as total suspended particulate since no size-selective inlet was employed. The flow rate was controlled at 30 L/min using a flowmeter, corresponding to a filter face velocity of approximately 0.288 m s^{-1}. Previous reports have indicated that the face velocity has negligible effect on the concentrations of sulphate, nitrate, and ammonium when using quartz filter for sampling (Keck and Wittmaack, 2005). To minimize the potential influence of the loose ground surface on the TSP collection, a mountain tent was used to separate the pump (out the tent) with the denuder-filter system (in the other side of tent), and the inlet Teflon tube was stretched out of the tent for ~1.5 m height straight.

From April 24th to May 6th, 2022, $PM_{2.5}$ were sampled using a high-volume aerosol sampler (TH-1000F; Wuhan Tianhong Instruments Co. Ltd., China) equipped with $PM_{2.5}$ inlet and Whatman quartz-fiber filters (sheets, 203 mm × 254 mm) at a flow rate of 1.5 m^3/min. All the quartz filters were pre-heated at 400 ℃ for 3 h before use. In general, TSP and $PM_{2.5}$ samples were collected with diurnal resolution during this campaign, with daytime samples from approximately 09:00–20:00 and nighttime samples from 21:00–08:00 (local time), respectively. From May 2nd to May 4th, we collected the daytime TSP and $PM_{2.5}$ samples in the morning (09:00-14:00) and afternoon (14:00-20:00), respectively. A total of 24 TSP samples (including 2 blanks) and 29 $PM_{2.5}$ (including 3 blanks) were collected during this campaign. After each sampling period, quartz filters were removed from the filter pack/$PM_{2.5}$ inlet and then stored in frozen until analysis. During the campaign, snowfall events occurred on the night of April 29th and during the daytime of April 30th.

Surface soil samples (n = 9) were collected on both sides of the Rongbuk valley (i.e., east and west) as well as on the south side in May, 2023. Soil samples were transported into laboratory using a cold chain. Upon arrival at our laboratory, soil samples were passed through a 60-mesh screen (~0.25 mm).

2.3 Ionic concentration analysis

Water-soluble inorganic ions (WSIs, including Na^+, NH_4^+, K^+, Mg^{2+}, Ca^{2+}, Cl^-, NO_2^-, NO_3^-, and

https://doi.org/10.5194/egusphere-2024-4165
Preprint. Discussion started: 16 January 2025

SO_4^{2-}) in TSP (entire filter, ~16.6 cm^2) and $PM_{2.5}$ (1/32 section, ~13.0 cm^2) were extracted using 20 mL Milli-Q water (18.2Ω cm) in an ultrasonic bath at room temperature for 30 min. After filtration through a 0.22 μm pore size syringe filter which was pre-cleaned with purewater, the extract was subjected to inorganic species analysis using ion chromatography (Dionex Aquion) (Zhang et al., 2020). Blank samples were pretreated and analyzed along with the aerosol samples. The ionic concentrations reported here were blank corrected (volatile components (i.e., NH_4^+, NO_2^-, NO_3^-) and K^+ in blank are always below the detection limits; SO_4^{2-}, Mg^{2+} and Ca^{2+} in blank are generally lower than samples by at least five times (the lower end); Na^+ in the blank is comparable to samples and was not presented in this study). The analysis uncertainties were typically within 5% standard deviation based on replicate measurements of standards (n = 10). The detection limit for the inorganic species is general less than 6 ng mL^{-1}.

For soil ionic concentration analysis, 4.0 g sieved soil was extracted using 20 mL Milli-Q purewater, shaken for 30min at room temperature. After centrifugation, the extract was passed through 0.45 mm filters before ions analysis. The concentration determination of water-soluble inorganic ions in soil extract was similar to that of aerosol samples. Detailed procedure for the extraction of soil inorganic ions, especially the NO_2^- has been descried in previous report (Homyak et al., 2015).

2.4 Isotopic analysis

After concentration measurements, isotopic analyses ($\delta^{15}N$, $\delta^{18}O$, and $\Delta^{17}O$) of NO_2^- in TSP were conducted using the azide method (Casciotti et al., 2007). The azide method can reduce nitrite ion in solution into N_2O in a single step, while nitrate ion remains unchanged, ensuring no interference on the nitrite isotopic analysis. The azide reagent is prepared by mixing 2 M sodium azide with 40% acetic acid at a 1:1 ratio by volume in our laboratory. NO_2^- standards and samples were pretreated under identical conditions concerning the total volume, nitrite amount, water isotope, and matrix. The $\delta^{15}N$, $\delta^{18}O$, and $\delta^{17}O$ of N_2O reduced from NO_2^- in the TSP samples and standards were determined using a Finnigan® MAT253 plus isotope ratio mass spectrometer (IRMS) equipped with a GasBench II and preconcentration system. The data calibration followed the procedures described in *Albertin et al.*, 2021, using three international KNO_2 salt standards (RSIL-N10219, RSIL-N7373, and RSIL-N23 with respective $\delta^{15}N$ and $\delta^{18}O$ values of 2.8/88.5 ‰, -79.6/4.2 ‰, and

https://doi.org/10.5194/egusphere-2024-4165
Preprint. Discussion started: 16 January 2025

3.7/11.4‰). The $\Delta^{17}O$ of RSIL-N7373 and RSIL-N23 are suggested to be zero (Albertin et al., 2021), while the $\Delta^{17}O$ of RSIL-N10219 is determined to be (-9.3 ± 0.2) ‰ in our laboratory. The ^{17}O-excess in samples is then calculated as $\Delta^{17}O = \delta^{18}O - 0.52 \times \delta^{17}O$. The standard deviations for $\delta^{15}N$, $\delta^{18}O$, $\Delta^{17}O$ of reference materials (n = 10) were determined to be less than 0.1‰, 0.6‰, and 0.4‰, respectively.

For soil NO_2^- isotopic analysis, ~30.0g sieved soil was extracted using 150 mL Milli-Q purewater. The soil extract was then preconcentrated into 10 mL using ion-exchange resin before isotopic analysis. The preconcentration approach was widely used for nitrate isotopic analysis in snow and ice samples, and the detailed procedures and the performance have been provided in *Erbland et al.,* 2013. The concentrated soil extracts (50 nmol NO_2^-) was then subjected to soil NO_2^- isotopic analysis by converting into N_2O via the azide method. The remaining procedures of soil NO_3^- and NO_2^- analysis were same as those for TSP samples, as aforementioned.

2.5 Complementary analyses of air mass backward trajectory

To evaluate the possible impact of biomass burning emissions or other pollution sources from South Asia, the Hybrid Single-Particle Lagrangian Integrated Trajectory (HYSPLIT) model (performed using TrajStat plugin of the MeteoInfo software) and archived Global Data Assimilation System (GDAS) of meteorological data were used to model the air mass back trajectories (Wang, 2014). In this study, six-day air mass backward trajectories with arriving height of 1000 m above ground level were simulated to identify the most likely pathway and potential source regions of the air masses at the Base Camp. Moreover, the Fire Information and Resource Management System (FIRMS) developed by Moderate Resolution Imaging Spectrometer (MODIS) (https://worldview.earthdata.nasa.gov) was employed to identify the distribution of active fire spots during the sampling period.

3 Results

3.1 Mass concentrations of water-soluble inorganic ions in TSP and $PM_{2.5}$

Figure 1 displays the chemical compositions of water-soluble inorganic ions, their corresponding time series and fractional contributions in TSP and $PM_{2.5}$. Throughout the campaign, substantial variations of total WSIs in $PM_{2.5}$ were observed, with a general decline after May 1st.

https://doi.org/10.5194/egusphere-2024-4165
Preprint. Discussion started: 16 January 2025

This decline was predominately driven by significant reductions in secondary inorganic species, i.e., SO_4^{2-}, NO_3^- and NH_4^+, with the magnitude by more than 60%. In particular, NH_4^+ in $PM_{2.5}$ declined from (322 ± 243) ng m^{-3} before May 1st to negligible after May 1st. Therefore, the fractional contribution of secondary inorganic species in $PM_{2.5}$ also decreased. Similarly, K^+ in $PM_{2.5}$, a good tracer of biomass burning (Ma et al., 2003), also declined significantly after May 1st. The elevated concentrations of WSIs before May 1st are comparable to previous reports at remote sites over the TP (i.e., Namco, QOMS) in the spring (Wang et al., 2020; Lin et al., 2020; Lin et al., 2021; Decesari et al., 2010). In comparison, concentrations of Ca^{2+} and Mg^{2+}, tracers of wind-blown dust (Wang et al., 2002), decreased by less than 20% after May 1st, with a smaller degree than secondary species. In general, SO_4^{2-}, NO_3^-, and Ca^{2+} are the most abundant species in $PM_{2.5}$, accounting for the majority of the mass of total WSIs. In addition, despite the average daytime concentrations of the inorganic species were generally higher than those at night, no clear diurnal variation was observed in this study.

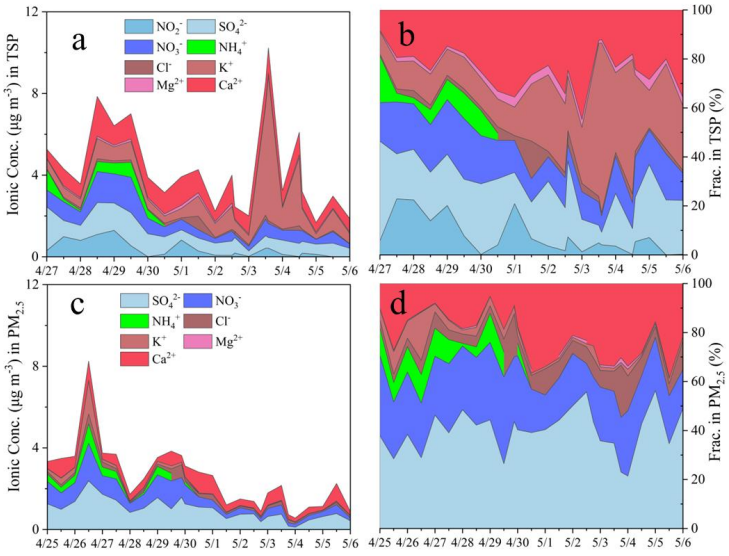

Figure 1. The chemical compositions and time series of mass concentrations of water-soluble inorganic species (NO_2^-, SO_4^{2-}, NO_3^-, Ca^{2+}, etc.), as well as the corresponding mass fractions in respective TSP (a, b) and $PM_{2.5}$ (c, d) samples collected at Base Camp of Mt. Qomolangma in spring 2022.

https://doi.org/10.5194/egusphere-2024-4165
Preprint. Discussion started: 16 January 2025

The variations of WSIs in TSP generally followed a similar pattern to that in $PM_{2.5}$ (Figure 1). For example, after May 1st, the secondary inorganic species in TSP declined considerably by over 50% (i.e., NH_4^+ in TSP declined by more than tenfold), while Ca^{2+} in TSP decreased with a smaller degree (< 15%) and Mg^{2+} remained stable. In contrast, TSP K^+ (from both crustal and biomass burning sources)(Hsu et al., 2009) drastically surged on May 3rd and May 4th. Note that other species in TSP, i.e., SO_4^{2-} and NO_3^- also increased to some extent on May 3rd.

The most distinct feature of chemical compositions in TSP was the elevated level and significant variation of NO_2^-, ranging from 0.2 ng m^{-3} to 1291 ng m^{-3} in air and with an average of 375 ± 386 ng m^{-3}. In comparison, NO_2^- consistently remained below the detection limit in $PM_{2.5}$ samples. Note during the laboratory measurements of ionic concentrations, TSP and $PM_{2.5}$ filters were extracted with purewater and it was the extraction analyzed by ion chromatography. To ensure fair comparisons, similar areas of filters were extracted with same volume of purewater, so that the extractions from the $PM_{2.5}$ filters should be more concentrated in atmospheric particulate species compared to that from the TSP filters, since $PM_{2.5}$ samples were collected at a much faster sampling speed (1.5 m^3 min^{-1} vs. 30 L min^{-1}) over the same sampling duration. Nevertheless, NO_2^- was detectable only in the extractions of TSP filter. The determined NO_2^- concentrations in TSP in this study (375 ± 386 ng m^{-3}) were higher than previous reports conducted in various remote sites, such as at QOMS station (~60 ng m^{-3} for TSP) (Bhattarai et al., 2023), at a forest site in the Southeast Tibet Plateau (~140 ng m^{-3} for TSP) (Bhattarai et al., 2019), in the middle hills of the central Himalayas (~210 ng m^{-3} for TSP) (Tripathee et al., 2021).

In particular, there was a dramatic decrease in TSP NO_2^- after May 1st, from a mean of (625 ± 457) ng m^{-3} to (147 ± 145) ng m^{-3}, in line with the declines in other secondary inorganic species. Over the course of the campaign, NO_2^- comprised approximately 8% of the total WSIs mass in TSP, while its contribution reached maximum of ~20% on April 27th and April 28th, being one of the most abundant components on the two days. In addition, there was a strong correlation between NO_2^- and NO_3^- throughout the campaign ($r = 0.75$, $p < 0.05$. Figure S1). Meanwhile, the mean mass ratio of NO_2^- to NO_3^- was ~50% throughout the campaign, but on several days (i.e., April 27th) NO_2^- concentrations significantly exceeded that of NO_3^-. Previous study also reported comparable NO_2^- and NO_3^- concentrations in at a forest site in the Southeast Tibet (summer:100 ng m^{-3} vs. 110 ng m^{-}

https://doi.org/10.5194/egusphere-2024-4165
Preprint. Discussion started: 16 January 2025

^{3}; winter: 180 ng m^{-3} vs. 270 ng m^{-3}) (Bhattarai et al., 2019).

3.2 Isotopic signatures of nitrite in TSP

Figure 2 presents the times series of $\delta^{15}N$, $\delta^{18}O$ and $\Delta^{17}O$ of NO_2^- in TSP, along with the NO_2^- concentrations. Similar to the variation trend of NO_2^- concentrations, NO_2^- isotopes varied in a wider range before May 1st, but became more stable afterward. For example, $\delta^{15}N(NO_2^-)$ ranged from -10.9 ‰ to 0.8 ‰, with a relatively large standard deviation before May 1st compared to that after May 1st ((-6.4 ± 4.3) ‰ vs. (-8.0 ± 0.7) ‰). The large variability in $\delta^{15}N(NO_2^-)$ before May 1st is predominately attributed to the two high values observed in daytime of April 27th and night of April 28th. Note that the two high $\delta^{15}N(NO_2^-)$ samples were also associated with relatively high NO_2^- mass concentrations but relatively low $\delta^{18}O(NO_2^-)$. In contrast to the declining trend of NO_2^- concentrations, the mean $\delta^{15}N(NO_2^-)$ values were comparable before and after May 1st. Relatively large variability was observed in TSP $\delta^{18}O(NO_2^-)$, ranging from -9.0‰ to 3.9‰ and with an average of (-3.4 ± 3.8) ‰. TSP $\Delta^{17}O(NO_2^-)$ varied within a narrow range from -0.2‰ to +0.7‰ and with a mean of (0.2 ± 0.3) ‰. During the campaign, no significant correlations were observed between $\delta^{15}N(NO_2^-)$ and the NO_2^- concentrations; while $\delta^{18}O(NO_2^-)$ appeared to be moderately correlated with the NO_2^- concentrations (Figure S2).

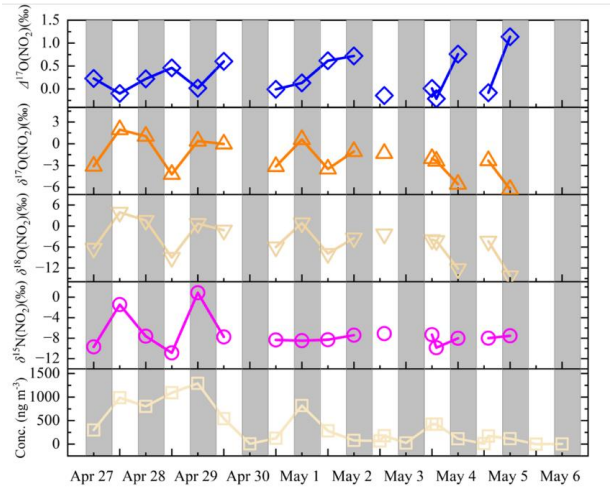

Figure 2. Time series of multiple isotopic signatures of NO_2^- ($\delta^{15}N$, $\delta^{18}O$, $\delta^{17}O$ and $\Delta^{17}O$) as well as corresponding concentrations in TSP samples during "Earth Summit Mission" scientific

https://doi.org/10.5194/egusphere-2024-4165
Preprint. Discussion started: 16 January 2025

expedition in spring 2022. The gray shaded area denotes local nighttime.

Table 1. The measured nitrite (and nitrate) concentration and isotopic signatures in surface soil collected in the Rongbuk Valley.

Soil sample ID	NO_2^-				NO_3^-			
	Conc.(ng g^{-1})	$\delta^{15}N$	$\delta^{18}O$	$\Delta^{17}O$	Conc.(ng g^{-1})	$\delta^{15}N$	$\delta^{18}O$	$\Delta^{17}O$
East-1	67.7	-12.0	6.1	3.3	1127.3	-2.7	23.4	5.7
East-2	76.1	-11.9	2.7	2.2	1098.3	1.3	18.1	3.8
East-3	82.3	-14.6	6.0	3.3	2978.1	-0.3	25.4	6.6
West-1	88.6	-10.1	8.9	1.6	3176.5	-3.1	44.5	13.4
West-2	106.2	-7.0	11.4	1.5	2880.3	-1.2	22.1	6.2
West-3	179.3	-5.2	12.7	1.4	7686.9	-3.4	35.8	11.4
South-1	53.8	-13.2	12.7	6.7	3651.2	-0.6	32.6	10.1
South-2	42.3	-9.0	18.1	7.3	1683.2	-2.2	49.3	14.8
South-3	48.9	-10.3	12.4	6.7	385.5	-2.4	45.7	14.9

3.3 Surface soil nitrite concentration and isotopic signature

The concentration of soil NO_2^- (and NO_3^-) as well as the corresponding isotopic signatures are displayed in Table 1. High soil NO_2^- and NO_3^- concentrations were observed on the west and east slopes of the Rongbuk valley relative to that on the south side of the sampling site. The mean surface soil NO_2^- and NO_3^- in the Rongbuk Valley were 82.8 and 2740.8 ng g^{-1}, respectively. The soil NO_3^- concentrations are significantly higher than the NO_2^- by a factor of 8 ~ 40. In general, the measured soil NO_3^- concentrations at the Rongbuk valley are significantly lower than other remote regions of TP (i.e., Naqu, Bangda), while soil NO_2^-concentrations are comparable to these reports (Wang et al., 2019). Soil $\delta^{15}N(NO_2^-)$ values ranged from -13.2‰ to -5.2‰ (on average -10.4‰), which are comparable to TSP $\delta^{15}N(NO_2^-)$. In comparison, we observed positive soil $\delta^{18}O(NO_2^-)$ and $\Delta^{17}O(NO_2^-)$, ranging from 2.7‰ to 18.1‰ (on average 10.5‰) and 1.4‰ to 7.3‰ (on average 3.8‰), respectively, in contrast to the negative $\delta^{18}O(NO_2^-)$ and near-zero $\Delta^{17}O(NO_2^-)$ observed in TSP samples. The determined soil $\delta^{18}O(NO_2^-)$ is comparable to that in laboratory incubated soil (11.8‰ ~ 12.5‰) (Lewicka-Szczebak et al., 2021).

4 Discussion

The significant contrast in NO_2^- concentrations between TSP and $PM_{2.5}$ samples, as shown in Figure 1, suggests that at the sampling site atmospheric particle NO_2^- overwhelmingly exists in coarse particles. This observation is consistent with previous studies across the TP, which also

https://doi.org/10.5194/egusphere-2024-4165
Preprint. Discussion started: 16 January 2025

reported the absence of NO_2^- in fine mode particles ($PM_{2.5}$ and $PM_{1.0}$) using either online real-time instrument or offline filter sampling (Decesari et al., 2010; Xu et al., 2020; Xu et al., 2023; Zhao et al., 2020), while relatively high levels of TSP NO_2^- have been reported (Bhattarai et al., 2019; Bhattarai et al., 2023; Tripathee et al., 2017). In general, the chemical sources of particle NO_2^- in the atmosphere encompass the uptake of HONO, particulate nitrate photolysis, and the NO_2-related reactions (i.e., photo-enhanced uptake of NO_2 on mineral dust, heterogeneous reaction of NO_2 on the surface of aerosol) (Nie et al., 2012; Vandenboer et al., 2014a; Chen et al., 2019; Shang et al., 2021), as summarized in Table 2. In addition to these in-situ atmospheric processes, growing evidence has revealed that long-range transport of atmospheric pollutants from South Asia also contributes considerably to aerosol loadings in TP in the spring (Kang et al., 2019; Bhattarai et al., 2023; Zhao et al., 2020), which may also bring nitrite along with other pollutants. Moreover, the lifting of surface dust can also contribute to the atmospheric coarse particles and significantly influence the chemical composition of TSP (Zhang et al., 2021a; Pokharel et al., 2019), and therefore soil nitrite could also be a potential source for TSP NO_2^-. In the following discussion, we examine the potential importance of the abovementioned processes to the observed high NO_2^- content in coarse particle and discern the most likely ones.

Table 2. Particulate nitrite concentration and formation pathways/sources compiled in the literature.

Site	Period	NO_2^- Conc. (mean, ng m^{-3})	Formation pathways/Sources	Reference
QOMS station	April 2017	60	Biomass burning emission transported from South Asia	Bhattarai et al., 2023
Bakersfield, California	May–July 2010	150	HONO uptake on lofted alkaline soil particles.	VandenBoer et al., 2014
Jinan, China	November 2013 − January 2014	2080	Heterogeneous reactions of NO_2	Wang et al., 2015
Seoul, Korea	May−July, 2005	1410	Heterogeneous reactions of NO_2	Song et al., 2009
Shanghai, China	June 2020	210	Heterogeneous reactions of NO_2, reduction of NO_2 by S(IV)	Shang et al., 2021
Mt.Heng, China	April 2009	2500	Surface TiO_2 photocatalysis of NO_2	Nie et al., 2012

4.1 The potential effects of atmospheric chemistry on NO_2^- in TSP

Increasing evidence supports particulate nitrate photolysis as an important source of atmospheric HONO especially in pristine atmosphere, with NO_2^- serving as the intermediate in the

https://doi.org/10.5194/egusphere-2024-4165
Preprint. Discussion started: 16 January 2025

subsequent gas-particle partition process (Andersen et al., 2023; Ye et al., 2016). In theory, particulate NO_2^- (and HONO) produced from particulate nitrate photolysis might be associated with extremely negative $\delta^{15}N$ values, due to the significant nitrogen isotopic fractionation effect during nitrate photolysis (Erbland et al., 2013). For example, NO_2^- in water of hypersaline ponds and soil of McMurdo Dry Valleys, Antarctica, produced from the NO_3^- photolysis, were characterized by significantly negative $\delta^{15}N$ values (< -80‰) (Peters et al., 2014). However, $\delta^{15}N(NO_2^-)$ in this study was only ~2‰ lower than the $\delta^{15}N(NO_3^-)$ in TSP samples collected during this campaign (on average (-5.3 ± 3.3)‰, Text S1) and that at the QOMS stations (annual average of (-5.1 ± 2.3) ‰) (Wang et al., 2020). The similarity in $\delta^{15}N$ isotopes between NO_2^- and NO_3^- suggests particulate nitrate photolysis is unlikely to be the primary source of the TSP NO_2^-.

In addition to nitrate photolysis, the absorption of HONO on alkaline aerosols (i.e., lofted dust and road salt particles) can also result in accumulation of NO_2^- into the particle phase (Vandenboer et al., 2014a; Chen et al., 2019). For example, *VandenBoer et al.* observed a synchronous enhancement of fine particle NO_2^- (as high as 730 ng m^{-3}) alongside the buildup of HONO (up to 1.37 ppbv) after sunset in an agricultural site (Vandenboer et al., 2014a). However, the levels of HONO in terrestrial background environments, typically on the order of dozens of pptv (Ye et al., 2023), are obviously too low to support the observed unexpectedly high levels of particulate NO_2^- (up to 1300 ng m^{-3}). What is more, previous studies indicted the HONO uptake predominately occurs on fine particles (Wang et al., 2015; Chen et al., 2019; Shang et al., 2021), while our observations indicated NO_2^- only exists in coarse particles.

The uptake of NO_2 on mineral dust has also been identified as a significant route for the formation of particulate NO_2^- or gas-phase HONO (Nie et al., 2012; Ndour et al., 2008). For example, *Nie et al.* found a significantly enhanced NO_2^- in coarse particle during daytime in a dust storm event in Mt. Heng (up to 4.5 μg m^{-3}) (Nie et al., 2012). The proposed mechanism is initialed by photocatalysis of NO_2 to NO_2^- via photo-produced electrons on surface of dust. Nevertheless, given the relatively small NO_2 uptake coefficients (generally lower than 10^{-6}) (Yu et al., 2021; Bao et al., 2022) and the low concentration of NO_2 in pristine environment of TP (e.g., ~ 140 pptv at Namco (Wang et al., 2023), and would be even lower at Mt. Qomolangma), such high levels of particulate NO_2^- are beyond the capacity of NO_2 heterogeneous reactions.

https://doi.org/10.5194/egusphere-2024-4165
Preprint. Discussion started: 16 January 2025

Other than the above-mentioned rationales, the atmospheric physicochemical processes leading to NO_2^- production would influence both fine and coarse-mode particles, and some of the processes (e.g., HONO uptake) preferentially interact with fine-mode particles. However, the observation indicated NO_2^- only exists in TSP but not $PM_{2.5}$, suggesting atmospheric physicochemical processes are unlikely to account for the elevated levels of NO_2^- in TSP.

4.2 Potential effect of biomass burning emissions in South Asia via long-range transport

There is a growing body of compelling evidence indicating that the elevated aerosol loadings and chemical species in TP during spring, i.e., black carbon (Cong et al., 2015; Kang et al., 2019) and soluble components (Dasari et al., 2023; Bhattarai et al., 2023; Lin et al., 2021; Wang et al., 2020; Zhao et al., 2020) are significantly linked to biomass burning emissions from South Asia, which can penetrate into TP via long range transport. Recently, *Bhattarai et al.* observed synchronously elevated water-soluble nitrogen compounds (i.e., NO_2^-, NH_4^+, NO_3^-), levoglucosan (a molecule marker for biomass burning) and bulk $\delta^{15}N$ signatures in TSP at QOMS station, once upon the arrival of biomass burning plumes from South Asia (Bhattarai et al., 2023). Specially, they found that TSP NO_2^- averaged 60 ng m^{-3} during the spring biomass burning influenced episodes, while NO_2^- was always below the detection limit in other seasons (Bhattarai et al., 2023). This suggests that biomass burning events in South Asia and the subsequent long-range transport could contribute to accumulation of NO_2^- in aerosols in Tibet.

To evaluate the potential effects of South Asian pollutants on our observations, we further analyzed the air masses origins during the sampling campaign. As shown in Figure 3, during the first-half of the campaign, i.e., before May 1st, air masses mainly originated from or pass through northern India and Nepal with intensive human activities and numerous fire hotspots, while from May 1st to May 6th the air masses originated from the inside of the TP with rare open fires. Accompanied by this shift in air mass origins, the concentrations of NH_4^+, NO_3^- and SO_4^{2-} in both $PM_{2.5}$ and TSP, as well as the TSP NO_2^- apparently decreased, suggesting that these species in $PM_{2.5}$ and TSP should be controlled or closely related to biomass burning events in South Asia and the subsequent long-range transport of biomass burning pollutants.

However, although biomass burning activities indeed emit various nitrogen compounds into

https://doi.org/10.5194/egusphere-2024-4165
Preprint. Discussion started: 16 January 2025

atmosphere, particle nitrite has not yet been detected in biomass burning plumes (Lindaas et al., 2021; Juncosa Calahorrano et al., 2021; Li et al., 2003). It is also difficult for the long-range transport to explain why NO_2^- is predominately present in coarse particles, as fine mode particle is typically easier to be transported in principle. Moreover, transport of pollutants from South Asia is also difficult to explain the presence of NO_2^- in TSP after May 1st when air mass mainly originated from clean regions with minor anthropogenic activities, i.e., the Central Tibet.

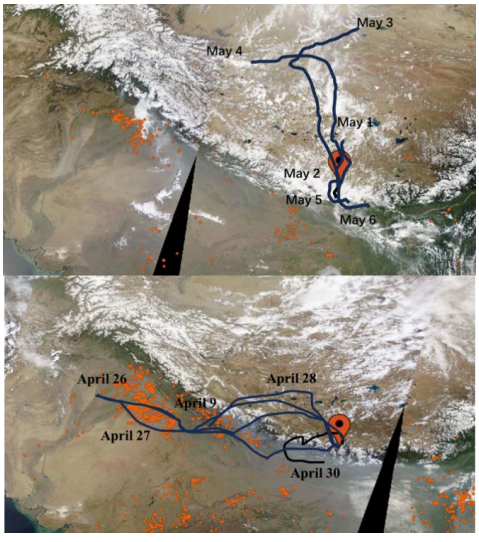

Figure 3. The modelled six-day air-mass back trajectories during "Earth Summit Mission" scientific expedition in spring 2022 (a: from May 1st to May 6th; b: April 26th to April 30th). The active fire spots captured by MODIS (https://worldview.earthdata.nasa.gov) are also presented.

4.3 The potential effects of lofted dust

Previous reports have confirmed that wind-blown mineral dust contributed significantly to coarse mode aerosols in TP (Kang et al., 2016; Zhang et al., 2021a). Notably, surface soil collected from the Rongbuk valley is characterized with elevated NO_2^- concentration (up to 180 ng g^{-1}, Table 1). The surface soil NO_2^- is expected to mainly reside in the coarse mode after suspended in the atmosphere (Drakaki et al., 2022), consistent with our observations that particle NO_2^- was predominately confined into coarse particle. The unique environment of Rongbuk valley, characterized by exposed surface soil and strong wind (reaching as high as 9 m/s during this

https://doi.org/10.5194/egusphere-2024-4165
Preprint. Discussion started: 16 January 2025

campaign) could facilitate the resuspension of soil components into the atmosphere. Furthermore, small localized tornadoes were frequently observed before May 1st, while the snow events occurred in April 30th would reduce the soil-derived dust emission by increasing the snow coverage and enriching the soil moisture. In fact, concentrations of Ca^{2+} in TSP, which predominately originate from dust emission, also declined to some extent after May 1st.

In addition, the similarity in $\delta^{15}N$ of NO_2^- between TSP and the surface soil (-7.3 ± 3.1‰ vs. -10.3 ± 3.0‰) also supports that locally emitted surface soil may contribute to the observed high levels of TSP NO_2^-. But one should note that the oxygen isotopes of TSP and soil NO_2^- are different. This could be explained by the potential oxygen isotope exchanges between NO_2^- and aerosol liquid water (fractionation effect of $^{18}\varepsilon_{eq} \approx 16‰$ at local temperature, T = 270K, $^{18}\varepsilon_{eq} = -0.12\ T + 48.79$ (Buchwald and Casciotti, 2013)), which will deplete the initial soil $\delta^{18}O(NO_2^-)$ once resuspended into atmosphere. The atmospheric water vapor $\delta^{18}O$ isotope in TP is determined to be significantly negative (approximately -35‰ to -15‰ at a remote site in TP with altitude of ~ 4200m) (Yu et al., 2015). The oxygen isotope exchange between NO_2^- and H_2O would also homogenize and erase original soil $\Delta^{17}O(NO_2^-)$ signals, because aerosol liquid water content is at least three orders of magnitude higher than NO_2^- (Text S2) and characterized by negligible $\Delta^{17}O$ values (Luz and Barkan, 2005).

We also noted that NO_2^- in surface soil is significantly lower than NO_3^-, by up to 40 times (Table 1), contrasting with the chemical compositions in TSP. Soil samples were sieved to less than 60 mesh (~250 μm), to be in similar order with the diameters of TSP. We speculate that the size distribution of NO_2^- in surface soil maybe different with NO_3^- if resuspended surface soil was the primary source of TSP.

5 Conclusion and Implications

Unexpectedly high levels of coarse-particle NO_2^- were observed in the pristine environment at Mt. Qomolangma in the spring, 2022. After examining the potential contributions of various NO_2^- sources with assistance from air mass back-trajectory and isotope analyses, we suggest that soil-derived nitrite likely serves as a baseline source of atmospheric NO_2^-, maintaining the background levels of TSP NO_2^- at this pristine site. Moreover, air masses originating from South Asia would

https://doi.org/10.5194/egusphere-2024-4165
Preprint. Discussion started: 16 January 2025

also contribute to elevated NO_2^- by bringing biomass burning pollutants, as evidenced by the observed higher TSP NO_2^- before May 1st compared to after that day when air mass origins shifted from South Asia to Central Tibet. The dual-contribution of soil nitrite and long-range transport of pollutants from South Asia to the observed TSP NO_2^- at Mt. Qomolangma is also consistent with the dynamics of NO_2^- isotopic signatures, as the isotopes were more varied during the first half of the campaign when both soil and long-range transport-related nitrite contributed, while in the second half of the campaign the isotopes were more stable when soil nitrite predominated. The effect of long-range transport from South Asia, however, would be likely mainly through the transport of nitrite precursors (e.g., NO_2, HONO) rather than nitrite itself as there is likely no nitrite in biomass burning plumes (Lindaas et al., 2021; Juncosa Calahorrano et al., 2021; Li et al., 2003). Nevertheless, it is currently unknown why such precursors would selectively interact with coarse mode particles, resulting in nitrite predominately resides in coarse-mode particles. Further investigation should be conducted to clarify the reason.

Our results highlight that soil nitrite could also be directly lofted into atmosphere and potentially acting as an important NO_x and HONO source, a previously unrecognized soil–atmosphere interactions which may greatly impact the atmospheric environment (Figure 4). The elevated levels of particle NO_2^- may serve as an important HONO source through the gas-to-particle partition process (Vandenboer et al., 2014a), and the thermodynamic equilibrium between particulate nitrite and HONO ([pN(III)]/[HONO] ratio) is primarily governed by the particle acidity and liquid water content (LWC) in theory (Fountoukis and Nenes, 2007; Vandenboer et al., 2014a; Chen et al., 2019). Based on the observed TSP NO_2^- and estimated ratio of [pN(III)]/[HONO] (from 4.8 to 10.6, Text S2), we can estimate the potential level of atmospheric HONO if the partition ever occurs at this site (Vandenboer et al., 2014b), and result indicates HOHO would be at 8 ~ 15 pptv, on the same order with the observations at a central Tibetan site (~ 30 pptv at Namco (Wang et al., 2023)). Therefore, we suspect that the elevated levels of particle NO_2^- by lofted soil may significantly impact local reactive nitrogen cycling and atmospheric oxidation capacity by acting as source of reactive nitrogen species through photolysis or thermodynamic partitioning processes in the pristine environment of TP (Li, 1994; Song et al., 2009; Wang et al., 2015; Chen et al., 2019).

https://doi.org/10.5194/egusphere-2024-4165
Preprint. Discussion started: 16 January 2025

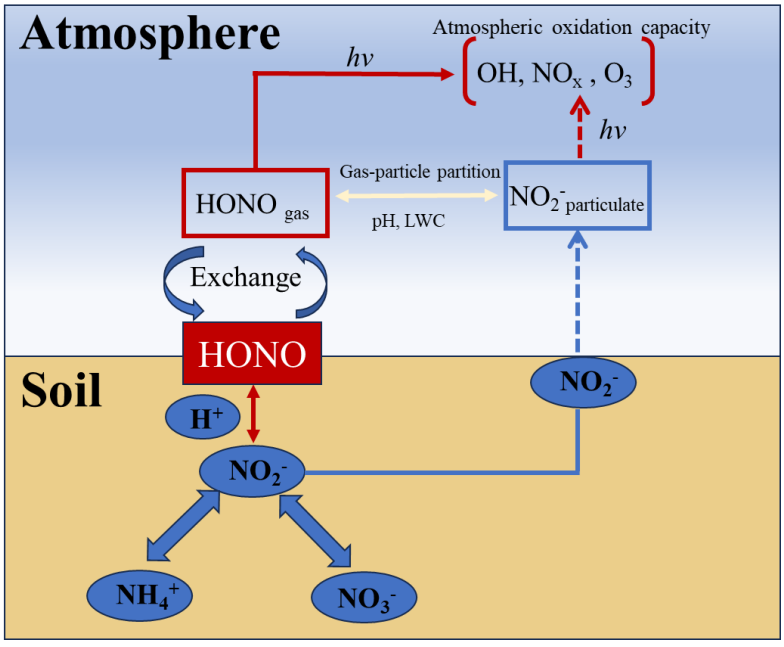

Figure 4 The conceptual model illustrating the impact of soil nitrite on the atmospheric reactive nitrogen cycling and atmospheric oxidation capacity. Through bi-direction exchange, soil nitrite is an important source of atmospheric HONO. Moreover, the wind-blown soil nitrite can also contribute to atmospheric HONO and NO_x through thermodynamic partition process or photolysis.

Acknowledgments We thank Dr. Yunhong Zhou for the help in air mass back trajectory analysis. The authors thank all researchers involved in the "Earth Summit Mission-2022" scientific expedition from Peking University, Hefei Institutes of Physical Science Anhui Institute of Optics and Fine Mechanics of Chinese Academy of Sciences, Minzu University of China.

Financial support L.G. acknowledges financial support from the National Natural Science Foundation of China (Awards: 41822605 and 41871051), and the National Key R&D Program of China (2022YFC3700701). Z. Z acknowledges financial support from the National Natural Science Foundation of China (Awards: 42273001). P. C acknowledges financial support from the National Natural Science Foundation of China (Awards: 42371151).

https://doi.org/10.5194/egusphere-2024-4165
Preprint. Discussion started: 16 January 2025

Conflicts of interest

The authors declare that they have no conflicts of interest.

Autor contribution:

L.G designed the research, interpreted the data; L.G and Z.Z prepared the manuscript with contributions from all co-authors; Z.Z., Y.W., C.Y., T.Z., C.Z., Z.J., and P.C., conducted the field sampling and laboratory measurements; L.G, Z.Z., and P.C., acquired funding; L.G., S.K., and C.Y. reviewed and edited the manuscript. All authors have given approval to the final version of the manuscript.

Data availability

The data supporting the findings of this study are available in the archival repository at: https://doi.org/10.6084/m9.figshare.28188320.v1

References

Albertin, S., Savarino, J., Bekki, S., Barbero, A., and Caillon, N.: Measurement report: Nitrogen isotopes ($\delta^{15}N$) and first quantification of oxygen isotope anomalies ($\Delta^{17}O$, $\delta^{18}O$) in atmospheric nitrogen dioxide, Atmos. Chem. Phys, 21, 10477-10497, 10.5194/acp-21-10477-2021, 2021.

Andersen, S. T., Carpenter, L. J., Reed, C., Lee, J. D., Chance, R., Sherwen, T., Vaughan, A. R., Stewart, J., Edwards, P. M., and Bloss, W. J. J. S. A.: Extensive field evidence for the release of HONO from the photolysis of nitrate aerosols, Sci. Adv., 9, eadd6266, 2023.

Bao, F., Cheng, Y., Kuhn, U., Li, G., Wang, W., Kratz, A. M., Weber, J., Weber, B., Pöschl, U., and Su, H.: Key Role of Equilibrium HONO Concentration over Soil in Quantifying Soil–Atmosphere HONO Fluxes, Environ. Sci. Tech., 56, 2204-2212, 10.1021/acs.est.1c06716, 2022.

Bhattarai, H., Wu, G., Zheng, X., Zhu, H., Gao, S., Zhang, Y.-L., Widory, D., Ram, K., Chen, X., and Wan, X.: Wildfire-Derived Nitrogen Aerosols Threaten the Fragile Ecosystem in Himalayas and Tibetan Plateau, Environ. Sci. Tech., 2023.

Bhattarai, H., Zhang, Y.-L., Pavuluri, C. M., Wan, X., Wu, G., Li, P., Cao, F., Zhang, W., Wang, Y., and Kang, S.: Nitrogen speciation and isotopic composition of aerosols collected at Himalayan forest (3326 m asl): seasonality, sources, and implications, Environ. Sci. Tech., 53, 12247-12256, 2019.

Buchwald, C. and Casciotti, K. L.: Isotopic ratios of nitrite as tracers of the sources and age of oceanic nitrite, Nat. Geosci., 6, 308-313, 10.1038/ngeo1745, 2013.

Casciotti, K. L., Böhlke, J. K., McIlvin, M. R., Mroczkowski, S. J., and Hannon, J. E.: Oxygen isotopes in nitrite: Analysis, calibration, and equilibration, Anal. Chem., 79, 2427-2436, 2007.

Chen, Q., Edebeli, J., McNamara, S. M., Kulju, K. D., May, N. W., Bertman, S. B., Thanekar, S., Fuentes, J. D., and Pratt, K. A.: HONO, Particulate Nitrite, and Snow Nitrite at a Midlatitude Urban Site during Wintertime, ACS Earth Space Chem., 3, 811-822, 10.1021/acsearthspacechem.9b00023, 2019.

Cong, Z., Kang, S., Kawamura, K., Liu, B., Wan, X., Wang, Z., Gao, S., and Fu, P.: Carbonaceous aerosols on the south edge of the Tibetan Plateau: concentrations, seasonality and sources, Atmos. Chem. Phys., 15, 1573-1584, 10.5194/acp-15-1573-2015, 2015.

https://doi.org/10.5194/egusphere-2024-4165
Preprint. Discussion started: 16 January 2025

503 Dasari, S., Paris, G., Pei, Q., Cong, Z., and Widory, D.: Tracing the origin of elevated springtime
504 atmospheric sulfate on the southern Himalayan-Tibetan plateau, Environmental Science: Advances, 2,
505 1110-1118, 2023.
506 Decesari, S., Facchini, M., Carbone, C., Giulianelli, L., Rinaldi, M., Finessi, E., Fuzzi, S., Marinoni, A.,
507 Cristofanelli, P., and Duchi, R. J. A. C.: Chemical composition of PM10 and PM1 at the high-altitude
508 Himalayan station Nepal Climate Observatory-Pyramid (NCO-P)(5079 m asl), Atmospheric Chemistry
509 Physics, 10, 4583-4596, 2010.
510 Drakaki, E., Amiridis, V., Tsekeri, A., Gkikas, A., Proestakis, E., Mallios, S., Solomos, S., Spyrou, C.,
511 Marinou, E., Ryder, C. L., Bouris, D., and Katsafados, P.: Modeling coarse and giant desert dust particles,
512 Atmos. Chem. Phys., 22, 12727-12748, 10.5194/acp-22-12727-2022, 2022.
513 Erbland, J., Vicars, W. C., Savarino, J., Morin, S., Frey, M. M., Frosini, D., Vince, E., and Martins, J. M.
514 F.: Air–snow transfer of nitrate on the East Antarctic Plateau Part 1: Isotopic evidence for a photolytically
515 driven dynamic equilibrium in summer, Atmos. Chem. Phys, 13, 6403-6419, 10.5194/acp-13-6403-2013,
516 2013.
517 Fang, Y., Koba, K., Wang, X., Wen, D., Li, J., Takebayashi, Y., Liu, X., and Yoh, M.: Anthropogenic
518 imprints on nitrogen and oxygen isotopic composition of precipitation nitrate in a nitrogen-polluted city
519 in southern China, Atmos. Chem. Phys., 11, 1313, 2011.
520 Felix, J. D. and Elliott, E. M.: Isotopic composition of passively collected nitrogen dioxide emissions:
521 Vehicle, soil and livestock source signatures, Atmos. Environ., 92, 359-366,
522 10.1016/j.atmosenv.2014.04.005, 2014.
523 Fountoukis, C. and Nenes, A.: ISORROPIA II: a computationally efficient thermodynamic equilibrium
524 model for K^+–Ca^{2+}–Mg^{2+}–NH_4^+–Na^+–SO_4^{2-}–NO_3^-–Cl^-–H_2O aerosols, Atmos. Chem. Phys, 7, 4639-
525 4659, 2007.
526 Geng, L., Alexander, B., Cole-Dai, J., Steig, E. J., Savarino, J., Sofen, E. D., and Schauer, A. J.: Nitrogen
527 isotopes in ice core nitrate linked to anthropogenic atmospheric acidity change, Proc. Natl. Acad. Sci. U.
528 S. A., 111, 5808-5812, 2014.
529 Hastings, M. G., Sigman, D. M., and Lipschultz, F.: Isotopic evidence for source changes of nitrate in
530 rain at Bermuda, J. Geophys. Res-Atmos., 108, 10.1029/2003jd003789, 2003.
531 Homyak, P. M., Vasquez, K. T., Sickman, J. O., Parker, D. R., and Schimel, J. P.: Improving nitrite
532 analysis in soils: Drawbacks of the conventional 2M KCl extraction, Soil Science Society of America
533 Journal, 79, 1237-1242, 2015.
534 Hsu, S. C., Liu, S. C., Huang, Y. T., Chou, C. C., Lung, S. C., Liu, T. H., Tu, J. Y., and Tsai, F.: Long-
535 range southeastward transport of Asian biosmoke pollution: Signature detected by aerosol potassium in
536 northern Taiwan, J. Geophys. Res-Atmos., 114, 2009.
537 Immerzeel, W. W., Van Beek, L. P., and Bierkens, M. F.: Climate change will affect the Asian water
538 towers, Science, 328, 1382-1385, 2010.
539 Jacobi, H.-W., Kleffmann, J. r., Villena, G., Wiesen, P., King, M., France, J., Anastasio, C., and Staebler,
540 R.: Role of nitrite in the photochemical formation of radicals in the snow, Environ. Sci. Tech., 48, 165-
541 172, 2014.
542 Juncosa Calahorrano, J. F., Lindaas, J., O'Dell, K., Palm, B. B., Peng, Q., Flocke, F., Pollack, I. B.,
543 Garofalo, L. A., Farmer, D. K., and Pierce, J. R.: Daytime oxidized reactive nitrogen partitioning in
544 western US wildfire smoke plumes, J. Geophys. Res-Atmos., 126, e2020JD033484, 2021.
545 Kang, S., Chen, P., Li, C., Liu, B., and Cong, Z.: Atmospheric aerosol elements over the inland Tibetan
546 Plateau: Concentration, seasonality, and transport, Aerosol Air Qual. Res., 16, 789-800, 2016.

https://doi.org/10.5194/egusphere-2024-4165
Preprint. Discussion started: 16 January 2025

Kang, S., Zhang, Q., Qian, Y., Ji, Z., Li, C., Cong, Z., Zhang, Y., Guo, J., Du, W., Huang, J., You, Q., Panday, A. K., Rupakheti, M., Chen, D., Gustafsson, Ö., Thiemens, M. H., and Qin, D.: Linking atmospheric pollution to cryospheric change in the Third Pole region: current progress and future prospects, Natl. Sci. Rev., 6, 796-809, 10.1093/nsr/nwz031, 2019.

Keck, L. and Wittmaack, K. J. A. E.: Effect of filter type and temperature on volatilisation losses from ammonium salts in aerosol matter, Atmos. Environ., 39, 4093-4100, 2005.

Kehrwald, N. M., Thompson, L. G., Tandong, Y., Mosley-Thompson, E., Schotterer, U., Alfimov, V., Beer, J., Eikenberg, J., and Davis, M. E.: Mass loss on Himalayan glacier endangers water resources, Geophys. Res. Lett., 35, 2008.

Lau, W. K., Kim, M.-K., Kim, K.-M., and Lee, W.-S.: Enhanced surface warming and accelerated snow melt in the Himalayas and Tibetan Plateau induced by absorbing aerosols, Environ. Res. Lett., 5, 025204, 2010.

Lewicka-Szczebak, D., Jansen-Willems, A., Müller, C., Dyckmans, J., and Well, R.: Nitrite isotope characteristics and associated soil N transformations, Scientific Reports, 11, 5008, 2021.

Li, J., Pósfai, M., Hobbs, P. V., and Buseck, P. R.: Individual aerosol particles from biomass burning in southern Africa: 2, Compositions and aging of inorganic particles, J. Geophys. Res-Atmos., 108, 2003.

Li, S. M.: Equilibrium of particle nitrite with gas phase HONO: Tropospheric measurements in the high Arctic during polar sunrise, J. Geophys. Res-Atmos., 99, 25469-25478, 1994.

Lin, Zhang, Y.-L., Yu, M., Fan, M.-Y., Xie, F., Zhang, W.-Q., Wu, G., Cong, Z., and Michalski, G.: Formation mechanisms and source apportionments of airborne nitrate aerosols at a Himalayan-Tibetan Plateau site: Insights from nitrogen and oxygen isotopic compositions, Environ. Sci. Tech., 55, 12261-12271, 2021.

Lin, M., Hattori, S., Wang, K., Kang, S., Thiemens, M. H., and Yoshida, N.: A complete isotope ($\delta^{15}N$, $\delta^{18}O$, $\Delta^{17}O$) investigation of atmospherically deposited nitrate in glacial-hydrologic systems across the Third Pole region, J. Geophys. Res-Atmos., 125, e2019JD031878, 2020.

Lin, W., Zhu, T., Song, Y., Zou, H., Tang, M., Tang, X., and Hu, J.: Photolysis of surface O_3 and production potential of OH radicals in the atmosphere over the Tibetan Plateau, J. Geophys. Res-Atmos., 113, 10.1029/2007jd008831, 2008.

Lindaas, J., Pollack, I. B., Garofalo, L. A., Pothier, M. A., Farmer, D. K., Kreidenweis, S. M., Campos, T. L., Flocke, F., Weinheimer, A. J., Montzka, D. D., Tyndall, G. S., Palm, B. B., Peng, Q., Thornton, J. A., Permar, W., Wielgasz, C., Hu, L., Ottmar, R. D., Restaino, J. C., Hudak, A. T., Ku, I. T., Zhou, Y., Sive, B. C., Sullivan, A., Collett, J. L., and Fischer, E. V.: Emissions of Reactive Nitrogen From Western U.S. Wildfires During Summer 2018, J. Geophys. Res-Atmos., 126, 10.1029/2020jd032657, 2021.

Liu, X.-Y., Koba, K., Koyama, L. A., Hobbie, S. E., Weiss, M. S., Inagaki, Y., Shaver, G. R., Giblin, A. E., Hobara, S., and Nadelhoffer, K.: Nitrate is an important nitrogen source for Arctic tundra plants, Proc. Natl. Acad. Sci. U. S. A., 115, 3398-3403, 2018.

Lüthi, Z., Škerlak, B., Kim, S.-W., Lauer, A., Mues, A., Rupakheti, M., and Kang, S.: Atmospheric brown clouds reach the Tibetan Plateau by crossing the Himalayas, Atmospheric Chemistry Physics, 15, 6007-6021, 2015.

Luz, B. and Barkan, E.: The isotopic ratios $^{17}O/^{16}O$ and $^{18}O/^{16}O$ in molecular oxygen and their significance in biogeochemistry, Geochim. Cosmochim. Ac., 69, 1099-1110, 2005.

Ma, Y., Weber, R., Lee, Y. N., Orsini, D., Maxwell-Meier, K., Thornton, D., Bandy, A., Clarke, A., Blake, D., and Sachse, G.: Characteristics and influence of biosmoke on the fine-particle ionic composition measured in Asian outflow during the Transport and Chemical Evolution Over the Pacific (TRACE-P)

https://doi.org/10.5194/egusphere-2024-4165
Preprint. Discussion started: 16 January 2025

experiment, J. Geophys. Res-Atmos., 108, 2003.
Miller, D. J., Chai, J., Guo, F., Dell, C. J., Karsten, H., and Hastings, M. G. J. G. R. L.: Isotopic composition of in situ soil NOx emissions in manure-fertilized cropland, 45, 12,058-012,066, 2018.
Ming, J., Zhang, D., Kang, S., and Tian, W.: Aerosol and fresh snow chemistry in the East Rongbuk Glacier on the northern slope of Mt. Qomolangma (Everest), J. Geophys. Res-Atmos., 112, 2007.
Morin, S., Savarino, J., Frey, M. M., Yan, N., Bekki, S., Bottenheim, J. W., and Martins, J. M.: Tracing the origin and fate of NOx in the Arctic atmosphere using stable isotopes in nitrate, Science, 322, 730-732, 10.1126/science.1161910, 2008.
Ndour, M., D'Anna, B., George, C., Ka, O., Balkanski, Y., Kleffmann, J., Stemmler, K., and Ammann, M.: Photoenhanced uptake of NO_2 on mineral dust: Laboratory experiments and model simulations, Geophys. Res. Lett., 35, 2008.
Nie, W., Wang, T., Xue, L., Ding, A., Wang, X., Gao, X., Xu, Z., Yu, Y., Yuan, C., and Zhou, Z.: Asian dust storm observed at a rural mountain site in southern China: chemical evolution and heterogeneous photochemistry, Atmos. Chem. Phys. , 12, 11985-11995, 2012.
Peters, B., Casciotti, K. L., Samarkin, V. A., Madigan, M. T., Schutte, C. A., and Joye, S. B.: Stable isotope analyses of NO_2^-, NO_3^-, and N_2O in the hypersaline ponds and soils of the McMurdo Dry Valleys, Antarctica, Geochim. Cosmochim. Ac., 135, 87-101, 2014.
Pokharel, M., Guang, J., Liu, B., Kang, S., Ma, Y., Holben, B. N., Xia, X. a., Xin, J., Ram, K., Rupakheti, D., Wan, X., Wu, G., Bhattarai, H., Zhao, C., and Cong, Z.: Aerosol Properties Over Tibetan Plateau From a Decade of AERONET Measurements: Baseline, Types, and Influencing Factors, J. Geophys. Res-Atmos., 124, 13357-13374, 10.1029/2019jd031293, 2019.
Shang, X., Kang, H., Chen, Y., Abdumutallip, M., Li, L., Li, X., Fu, H., Wang, X., Wang, L., and Wang, X.: $PM_{1.0}$-nitrite heterogeneous formation demonstrated via a modified versatile aerosol concentration enrichment system coupled with ion chromatography, Environ. Sci. Tech., 55, 9794-9804, 2021.
Song, C. H., Park, M. E., Lee, E. J., Lee, J. H., Lee, B. K., Lee, D. S., Kim, J., Han, J. S., Moon, K. J., and Kondo, Y.: Possible particulate nitrite formation and its atmospheric implications inferred from the observations in Seoul, Korea, Atmos. Environ., 43, 2168-2173, 10.1016/j.atmosenv.2009.01.018, 2009.
Tripathee, L., Kang, S., Rupakheti, D., Cong, Z., Zhang, Q., and Huang, J.: Chemical characteristics of soluble aerosols over the central Himalayas: insights into spatiotemporal variations and sources, Environmental Science and Pollution Research, 24, 24454-24472, 2017.
Tripathee, L., Kang, S., Chen, P., Bhattarai, H., Guo, J., Shrestha, K. L., Sharma, C. M., Sharma Ghimire, P., and Huang, J.: Water-soluble organic and inorganic nitrogen in ambient aerosols over the Himalayan middle hills: Seasonality, sources, and transport pathways, Atmos. Res., 250, 10.1016/j.atmosres.2020.105376, 2021.
VandenBoer, T., Markovic, M., Sanders, J., Ren, X., Pusede, S., Browne, E., Cohen, R., Zhang, L., Thomas, J., and Brune, W.: Evidence for a nitrous acid (HONO) reservoir at the ground surface in Bakersfield, CA, during CalNex 2010, J. Geophys. Res-Atmos., 119, 9093-9106, 2014a.
VandenBoer, T. C., Young, C. J., Talukdar, R. K., Markovic, M. Z., Brown, S. S., Roberts, J. M., and Murphy, J. G.: Nocturnal loss and daytime source of nitrous acid through reactive uptake and displacement, Nat. Geosci., 8, 55-60, 10.1038/ngeo2298, 2014b.
Wang, J., Zhang, Y., Zhang, C., Wang, Y., Zhou, J., Whalley, L. K., Slater, E. J., Dyson, J. E., Xu, W., Cheng, P., Han, B., Wang, L., Yu, X., Wang, Y., Woodward-Massey, R., Lin, W., Zhao, W., Zeng, L., Ma, Z., Heard, D. E., and Ye, C.: Validating HONO as an Intermediate Tracer of the External Cycling of Reactive Nitrogen in the Background Atmosphere, Environ Sci Technol, 57, 5474-5484,

https://doi.org/10.5194/egusphere-2024-4165
Preprint. Discussion started: 16 January 2025

10.1021/acs.est.2c06731, 2023.

Wang, K., Hattori, S., Kang, S., Lin, M., and Yoshida, N.: Isotopic constraints on the formation pathways and sources of atmospheric nitrate in the Mt. Everest region, Environ. Pollut., 267, 115274, 2020.

Wang, L., Wen, L., Xu, C., Chen, J., Wang, X., Yang, L., Wang, W., Yang, X., Sui, X., and Yao, L.: HONO and its potential source particulate nitrite at an urban site in North China during the cold season, Sci. Total. Environ., 538, 93-101, 2015.

Wang, S., Liu, W., Zhao, S., Wang, C., Zhuang, L., Liu, L., Wang, W., Lu, Y., Li, F., and Zhu, G.: Denitrification is the main microbial N loss pathway on the Qinghai-Tibet Plateau above an elevation of 5000 m, Sci. Total. Environ., 696, 133852, 2019.

Wang, Y. Q. J. M. A.: MeteoInfo: GIS software for meteorological data visualization and analysis, Meteorol. Appl, 21, 360-368, 2014.

Wang, Z., Akimoto, H., and Uno, I.: Neutralization of soil aerosol and its impact on the distribution of acid rain over east Asia: Observations and model results, J. Geophys. Res-Atmos., 107, ACH 6-1-ACH 6-12, 2002.

Xu, B., Cao, J., Hansen, J., Yao, T., Joswia, D. R., Wang, N., Wu, G., Wang, M., Zhao, H., and Yang, W.: Black soot and the survival of Tibetan glaciers, Proc. Natl. Acad. Sci. U. S. A., 106, 22114-22118, 2009.

Xu, J., Hettiyadura, A. P. S., Liu, Y., Zhang, X., Kang, S., and Laskin, A.: Regional differences of chemical composition and optical properties of aerosols in the Tibetan Plateau, J. Geophys. Res-Atmos., 125, e2019JD031226, 2020.

Xu, J., Zhang, X., Zhao, W., Zhai, L., Zhao, M., Shi, J., Sun, J., Liu, Y., Xie, C., Tan, Y., Li, K., Ge, X., Zhang, Q., and Kang, S.: High-resolution physicochemical dataset of atmospheric aerosols over the Tibetan Plateau and its surroundings, Earth Syst. Sci. Data Discuss., 2023, 1-45, 10.5194/essd-2023-506, 2023.

Yao, T., Thompson, L. G., Mosbrugger, V., Zhang, F., Ma, Y., Luo, T., Xu, B., Yang, X., Joswiak, D. R., and Wang, W.: Third pole environment (TPE), Environ. Dev., 3, 52-64, 2012.

Ye, C., Zhou, X., Zhang, Y., Wang, Y., Wang, J., Zhang, C., Woodward-Massey, R., Cantrell, C., Mauldin, R. L., Campos, T., Hornbrook, R. S., Ortega, J., Apel, E. C., Haggerty, J., Hall, S., Ullmann, K., Weinheimer, A., Stutz, J., Karl, T., Smith, J. N., Guenther, A., and Song, S.: Synthesizing evidence for the external cycling of NOx in high- to low-NOx atmospheres, Nat. Commun., 14, 10.1038/s41467-023-43866-z, 2023.

Ye, C., Zhou, X., Pu, D., Stutz, J., Festa, J., Spolaor, M., Tsai, C., Cantrell, C., Mauldin, R. L., 3rd, Campos, T., Weinheimer, A., Hornbrook, R. S., Apel, E. C., Guenther, A., Kaser, L., Yuan, B., Karl, T., Haggerty, J., Hall, S., Ullmann, K., Smith, J. N., Ortega, J., and Knote, C.: Rapid cycling of reactive nitrogen in the marine boundary layer, Nature, 532, 489-491, 10.1038/nature17195, 2016.

Yu, C., Wang, Z., Ma, Q., Xue, L., George, C., and Wang, T.: Measurement of heterogeneous uptake of NO_2 on inorganic particles, sea water and urban grime, J. Environ. Sci, 106, 124-135, 2021.

Yu, W., Tian, L., Ma, Y., Xu, B., and Qu, D.: Simultaneous monitoring of stable oxygen isotope composition in water vapour and precipitation over the central Tibetan Plateau, Atmos. Chem. Phys, 15, 10251-10262, 10.5194/acp-15-10251-2015, 2015.

Zhang, L., Tang, C., Huang, J., Du, T., Guan, X., Tian, P., Shi, J., Cao, X., Huang, Z., and Guo, Q.: Unexpected high absorption of atmospheric aerosols over a western Tibetan Plateau site in summer, J. Geophys. Res-Atmos., 126, e2020JD033286, 2021a.

Zhang, Y.-L., Zhang, W., Fan, M.-Y., Li, J., Fang, H., Cao, F., Lin, Y.-C., Wilkins, B. P., Liu, X., Bao, M., Hong, Y., and Michalski, G.: A diurnal story of $\Delta^{17}O(NO_3^-)$ in urban Nanjing and its implication for

https://doi.org/10.5194/egusphere-2024-4165
Preprint. Discussion started: 16 January 2025

nitrate aerosol formation, npj Clim. Atmos. Sci., 5, 10.1038/s41612-022-00273-3, 2022.

Zhang, Z., Jiang, Z., Guan, H., Liang, Y., Zheng, N., and Guo, W.: Isotopic evidence for the high contribution of wintertime photochemistry to particulate nitrate formation in Northern China, J. Geophys. Res-Atmos., 126, e2021JD035324, 2021b.

Zhang, Z., Zeng, Y., Zheng, N., Luo, L., Xiao, H., and Xiao, H.: Fossil fuel-related emissions were the major source of NH_3 pollution in urban cities of northern China in the autumn of 2017, Environ. Pollut., 113428, 2020.

Zhao, C., Yang, Y., Fan, H., Huang, J., Fu, Y., Zhang, X., Kang, S., Cong, Z., Letu, H., and Menenti, M.: Aerosol characteristics and impacts on weather and climate over the Tibetan Plateau, Natl. Sci. Rev., 7, 492-495, 2020.

Zhou, L., Zou, H., Ma, S., Li, P., Zhu, J., and Huo, C.: Vertical air mass exchange driven by the local circulation on the northern slope of Mount Everest, Adv. Atmos. Sci., 28, 217-222, 2011.

Zhou, T., Jiang, Z., Zhou, J., Zhao, W., Wu, Y., Yu, H., Li, W., Zhang, Z., Su, G., Ma, T., and Geng, L.: Fast and Efficient Atmospheric NO_2 Collection for Isotopic Analysis by a 3D-Printed Denuder System, Anal. Chem., 94, 13215-13222, 10.1021/acs.analchem.2c02839, 2022.

Zhu, T., Lin, W., Song, Y., Cai, X., Zou, H., Kang, L., Zhou, L., and Akimoto, H.: Downward transport of ozone-rich air near Mt. Everest, Geophys. Res. Lett., 33, 2006.

Zong, Z., Sun, Z., Xiao, L., Tian, C., Liu, J., Sha, Q., Li, J., Fang, Y., Zheng, J., and Zhang, G.: Insight into the Variability of the Nitrogen Isotope Composition of Vehicular NOx in China, Environ. Sci. Tech., 54, 14246-14253, 10.1021/acs.est.0c04749, 2020.

Zou, H., Zhou, L., Ma, S., Li, P., Wang, W., Li, A., Jia, J., and Gao, D.: Local wind system in the Rongbuk Valley on the northern slope of Mt. Everest, Geophys. Res. Lett., 35, https://doi.org/10.1029/2008GL033466, 2008.